



Published in final edited form as:

J Mol Cell Cardiol. 2020 August ; 145: 112–121. doi:10.1016/j.yjmcc.2020.06.006.

Exogenous IL-4 shuts off pro-inflammation in neutrophils while stimulating anti-inflammation in macrophages to induce neutrophil phagocytosis following myocardial infarction

Michael J. Daseke II^{a,b,f}, Mavis A.A. Tenkorang-Impraim^a, Yonggang Ma^c, Upendra Chalise^{a,f}, Shelby R. Konfrst^{a,f}, Michael R. Garrett^d, Kristine Y. DeLeon-Pennell^{e,g}, Merry L. Lindsey^{a,f,*}

^aDepartment of Cellular and Integrative Physiology, Center for Heart and Vascular Research, University of Nebraska Medical Center, Omaha, NE, USA

^bDepartment of Physiology and Biophysics, University of Mississippi Medical Center, Jackson, MS, USA

^cDepartment of Molecular Pharmacology and Physiology, University of South Florida, Tampa, FL, USA

^dDepartment of Pharmacology, University of Mississippi Medical Center, Jackson, MS, USA

^eRalph H. Johnson Veterans Affairs Medical Center, Charleston, SC, USA

^fResearch Service, Nebraska-Western Iowa Health Care System, Omaha, NE, USA

^gDivision of Cardiology, Department of Medicine, Medical University of South Carolina, Charleston, SC 29425, USA

Abstract

Introduction: Macrophages and neutrophils are primary leukocytes involved in the inflammatory response to myocardial infarction (MI). While interleukin (IL)-4 is an in vitro anti-inflammatory stimulus, the MI myocardium does not express a considerable amount of IL-4 but does express IL4 receptors. We hypothesized that continuous exogenous IL-4 infusion starting 24 h after MI would promote a polarization switch in inflammatory cells towards a reparative phenotype.

Methods: C57BL/6J male mice (3–6 months of age) were subcutaneously infused with either saline ($n = 17$) or IL-4 (20 ng/g/day; $n = 17$) beginning 24 h after MI and evaluated at MI day 3.

Published by Elsevier Ltd. This is an open access article under the CC BY-NC-ND license (<http://creativecommons.org/licenses/by-nc-nd/4.0/>).

*Corresponding author at: Department of Cellular and Integrative Physiology, University of Nebraska Medical Center, Nebraska Medical Center, Omaha, NE, USA. Merry.Lindsey@unmc.edu (M.L. Lindsey).

Author contributions

MLL was responsible for the experimental design. All authors took part in performing experiments, drafting results sections, and editing the manuscript. All authors have reviewed and approved the article. All authors have no potential conflicts of interest to disclose.

Supplementary data to this article can be found online at <https://doi.org/10.1016/j.yjmcc.2020.06.006>.

Disclosures

All authors have read the journal authorship agreement and policy on disclosure of potential conflicts of interest and have nothing to disclose.

Results: Macrophages and neutrophils were isolated ex vivo from the infarct region and examined. Exogenous IL-4 decreased pro-inflammatory *Ccl3*, *Il12a*, *Tnfa*, and *Tgfb1* in neutrophils and increased anti-inflammatory Arg1 and Ym1 in macrophages (all $p < .05$). Tissue clearance by IL-4 treated neutrophils was not different, while selective phagocytosis of neutrophils doubled in IL-4 treated macrophages ($p < .05$). Of 24,339 genes examined by RNA-sequencing, 2042 genes were differentially expressed in macrophages from IL-4 stimulated infarct (all FDR $p < .05$). *Pdgfc* gene expression was ranked first, increasing 3-fold in macrophages stimulated with IL-4 ($p = 1 \times 10^{-9}$). Importantly, changes in macrophage physiology and transcriptome occurred in the absence of global LV effects. Bone marrow derived monocytes stimulated with mouse recombinant PDGF-CC protein (10 $\mu\text{g/ml}$) or PDGF-CC blocking antibody (200 ng/ml) did not change Arg1 or Ym1 expression, indicating the in vivo effect of IL-4 to stimulate macrophage anti-inflammatory gene expression was independent of PDGF-CC.

Conclusions: Our results indicate that exogenous IL-4 promotes inflammation resolution by turning off pro-inflammation in neutrophils while stimulating anti-inflammation in macrophages to mediate removal of apoptotic neutrophils.

Keywords

IL-4; Myocardial infarction; Cardiac repair; Phagocytosis; Macrophage; Inflammation

1. Introduction

Wound healing after myocardial infarction (MI) involves inflammatory and extracellular matrix (ECM) coordination to remove necrotic myocytes and generate an infarct scar. Pro-inflammation is the upregulation of pro-inflammatory genes (e.g. *Il1b*) in macrophages and neutrophils, whereas anti-inflammation is the upregulation of anti-inflammatory genes (e.g. *Arg1*) in macrophages and neutrophils. Interleukin (IL)-4 promotes an enhanced M2 anti-inflammatory phenotype when used in vitro to stimulate a variety of cell types [1–4]. IL-4 mRNA is not dramatically elevated in the left ventricle (LV) infarct region after MI in the rat [5]. In macrophages isolated ex vivo from mouse MI LV, IL-4 receptor alpha (*IL-4Ra*) increases at day (d) 3 and d7 [6]. IL4-induced gene-1 (*IL-4i1*) expression increases in macrophages at MI d1, and its role in facilitating the shift in macrophage polarization from M1 to M2 phenotype is seen at MI d3 [7]. In cardiac fibroblasts isolated ex vivo from MI LV, *IL-4Ra* increases at d3 and begins to decline at d7 [8]. This indicates that while IL-4 may not be endogenously produced in the MI LV, macrophages and fibroblasts upregulate the receptor and are likely highly responsive to IL-4 treatment [6,8]. Because IL-4 is efficacious in treating other inflammatory diseases such as rheumatoid arthritis, there is potential for IL-4 to serve as an exogenous protectant in MI wound healing [9,10].

Exogenous IL-4 treatment initiated by intraperitoneal (i.p.) injection at 2 days prior to MI or immediately before MI surgery prevented the need for cardiac repair and function by limiting necrosis necessitating the conversion to M1 early and to M2 macrophages at MI d7 [1]. Exogenous IL-4 administered i.p. at 20 min after ligation promoted anti-inflammation and prevented cardiac remodeling by increasing the expression of anti-inflammatory markers and decreasing infarct size to preserve LV infarct wall thickness and geometry [2]. There are no currently approved pre-treatments for MI, and peri-MI treatments given 30 min

after onset of ischemia are logistically not feasible for the majority of patients with MI. In addition, pre- and peri-MI treatments demonstrate effects of prevention, rather than mechanisms of MI response. For this reason, we chose an experimental paradigm where MI is given and treatment is started after neutrophil infiltration is invoked. We hypothesized that continuous exogenous IL-4 administration started 24 h after MI would promote a polarization switch in inflammatory cell phenotypes. The novelty of this study is that IL-4 treatment given in a translational protocol could provide a clinically relevant target for the treatment of MI by regulating neutrophil and macrophage polarization.

2. Methods

2.1. Mice

All animal procedures were conducted according to the Guide for the Care and Use of Laboratory Animals (Eighth edition, 2011), and all protocols were approved by the Institutional Animal Care and Use Committee at the University of Mississippi Medical Center or the University of Nebraska Medical Center. Male C57BL/6J wild-type mice (3–6 months old) were purchased from Jackson Laboratory and housed in the animal facility. We have previously shown sex differences in neutrophil responses to MI [11]. For this reason, we used male mice. All mice were maintained together in the same room, under a 12:12 h light-dark cycle and given ad libitum access to standard mouse chow and water.

Permanent left anterior coronary artery ligation surgery was performed according to guidelines using minimally invasive techniques as previously described to generate permanent occlusion MI [6,8,12–14]. We have previously reported that there is little to no influx of neutrophils in sham surgery performed with the minimally invasive approach [15]. Mice were given buprenorphine (0.5 mg/kg, i.p.) before surgery. MI was confirmed at the time of surgery by visual inspection of blanching of the LV and presence of ST segment elevation on EKG. Qualitative echocardiography was used to re-confirm MI 24 h later, and all mice were subcutaneously infused at that time with either saline or IL-4 (20 ng/g/day) via osmotic mini-pumps. IL-4 dose was determined from previous studies [2]. Mice were randomly selected for treatment and all procedures and analysis were performed in a blinded manner. Saline treated MI mice served as the positive MI controls.

2.2. Echocardiography

LV physiology was evaluated by 2-D echocardiography using a Vevo 2100 system (VisualSonics, Toronto, ON, Canada) as previously described, and according to the guidelines for measuring cardiac physiology in mice [16,17]. Mice were anesthetized with 1–2% isoflurane mixed in oxygen. Body temperature and heart rate were constantly monitored. Echocardiograms were obtained prior to MI (baseline d0) and at d3 MI in serial for the same mice. Measurements were analyzed in B-mode for long axis views and M-mode for short axis views. LV dimensions were calculated as averages of images from three cardiac cycles.

2.3. Tissue harvest and infarct size evaluation

Mice were euthanized at d3 MI using isoflurane (5%, inhalational). The hearts were flushed with cardioplegic solution (NaCl, 69 mM; NaHCO₃, 12 mM; glucose, 11 mM; 2,3-butanedione monoxime, 30 mM; EGTA, 10 mM; Nifedipine, 0.001 mM; KCl, 50 mM) to arrest the heart in diastole. Hearts were excised, and the LV was separated from the right ventricle [15,16,18]. The LV and right ventricle were individually weighed, and the LV was cut into three parts: base, middle and apex. The hearts were incubated in warm (37 °C) 1% 2, 3, 5-triphenyltetrazolium chloride (Sigma) for 5 min and imaged for determination of infarct area. Adobe Photoshop was used to calculate LV infarct (LVI) as a percentage of total LV area [14,19]. The LVI, which included the infarct region and border zone, was separated from the non-infarct remote (LVC) and both were individually snap frozen and stored in -80 °C. The middle piece was fixed in 10% zinc formalin for histology.

2.4. MI cell isolation

At d3 MI, neutrophils and macrophages were isolated from the LVI as previously described [6,8,13,20]. We have previously reported that both macrophages and neutrophils each comprise approximately 5% of the resident cardiac cell pool [6,13,21,22].

The LVI was rinsed with PBS and placed in a collagenase solution (600 U/mL Collagenase II + 60 U/mL DNase I) for digestion at 37 °C. The cell suspension was applied over pre-separation filters (130-041-407, 30 µm, Miltenyi Biotec, Bergisch, Gladbach, Germany) to obtain single cell suspension. Red blood cell lysis buffer (Miltenyi Biotec) was added to the suspension to break down erythrocytes. The single cell suspension was centrifuged at 300 xg for 10 min, and the cell pellet was resuspended in PEB buffer (PBS containing 2 mM EDTA and 0.5% BSA). For neutrophil isolation, cells were incubated with anti-Ly-6G MicroBeads Ultrapure for 10 min at 4 °C (Miltenyi Biotec, #130-120-337) and separated using a MiniMACS magnetic separator column. The positive selection contained Ly-6G⁺ neutrophils. For macrophage isolation, the Ly6G negative cells were incubated with CD11b microbeads (Miltenyi Biotec, 130-049-601) and further separated with MiniMACS magnetic separator column. The positive selection contained Ly-6G⁻/CD11b⁺ macrophages. Supplemental Fig. 1 shows the purity of the isolated MI macrophages.

2.5. Quantitative RT-PCR

Total RNA was extracted from neutrophils and macrophages using TRIzol Reagent (Invitrogen Life Technologies, Grand Island, NY, USA) and reverse transcribed into cDNA using the C1000 Touch thermal cycler (BioRad) [18,23]. Quantitative real-time PCR (qRT-PCR) was performed with cDNA serving as a template. The gene expression of 7 pro-inflammatory or pro-fibrotic and 4 anti-inflammatory markers (pro: *Ccl3*, *Ccl5*, *Il1b*, *Il6*, *Il12a*, *Tgfb1*, and *Tnfa* and anti: *Arg1*, *Il10*, *Mrc1*, and *Ym1*) in isolated neutrophils and macrophages was measured using High Capacity RNA-to-cDNA Kit (4837406, Applied Biosystems) and gene expression master mix (4369016, Applied Biosystems). M1 and N1 are simplistic labels to depict pro-inflammatory macrophage or neutrophil subtypes more active in the inflammatory phase of MI, whereas M2 and N2 are labels to define anti-inflammatory macrophages or neutrophils more active in the repair phase of MI. The effects of in vivo IL-4 stimulation on other common M1 and M2 markers are graphed in

Supplemental Fig. 2 [24]. PCR amplification was performed under the following cycling conditions: denaturation: 95 °C for 10 min; amplification: 40 cycles of 95 °C for 15 s and 60 °C for 60 s. The hypoxanthine guanine phosphoribosyl transferase 1 (*Hprt1*) gene was used as the reference gene and cycle threshold (Ct) values of the target genes were normalized to corresponding Ct values of *Hprt1*. Data are reported as 2^{-CT} values. Neutrophils were collected for qRT-PCR and macrophage samples were collected for RNA-seq. After RNA-seq, validation by qRT-PCR was performed on macrophage samples, with only $n = 4$ samples having sufficient mRNA left for the qRT-PCR experiments.

2.6. Tissue clearance assay

C57BL/6J male mice were subcutaneously infused with either saline ($n = 6$) or IL-4 (20 ng/g/day; $n = 7$) beginning 24 h after MI. Neutrophils were isolated ex vivo from d3 LV infarcts and plated in 48-well plates coated with 0.1% gelatin at a density of 1.0×10^5 cells/well. The cells incubated with the gelatin for 4 h at 37 °C after which the cells were removed. The wells were stained with Coomassie blue for 15 min to stain the remaining gelatin, and absorbance measured at 595 nm as described previously [11]. The negative control was wells with no cells. The percentage of tissue clearance was calculated by normalizing absorbance of the negative controls using the following formula: $1 - [(\text{sample Abs}) / (\text{negative control Abs})]$.

2.7. Ex vivo phagocytosis assay

Phagocytosis assay was performed as previously described [17]. MI mice treated with either saline ($n = 6$) or IL-4 (20 ng/g/day $n = 6$) by osmotic mini-pumps were sacrificed at d3 MI and macrophages isolated from the infarct regions. The macrophages were immediately fixed in 4% paraformaldehyde for 1 h and placed in 70% ethanol. Cells were plated on glass coverslips and stained for phagocytosis of myocytes using α -actinin rabbit monoclonal antibody (myocyte marker, 1:50, cell signaling technology, CST #6487S) followed by Texas (Tx) Red conjugated secondary antibody. Similarly, macrophages were stained for phagocytosis of neutrophils using rat anti-mouse Ly-6B.2 (neutrophil marker, 1:100, CL8993AP, Cedarlane) followed by fluorescein iso-thiocyanate (FITC) conjugated secondary antibody. DAPI dye was applied to stain macrophage nuclei. Image analysis was performed to determine co-localized staining between macrophages and myocytes or macrophages and neutrophils [17]. The data are presented as TxRed intensity score for the myocyte phagocytosis index and FITC intensity score to indicate the neutrophil phagocytosis index.

2.8. Macrophage transcriptomics

To determine the effect of IL-4 on d3 MI macrophages, whole-transcriptome analysis by RNA sequencing (RNA-seq) was performed [25,26]. Sample quality was evaluated and used to develop RNA libraries ($n = 21$ pooled index samples) using the TruSeq Stranded Total RNA with Ribo-Zero Kit, Set A (FC-122–2501, San Diego, CA) following manufacturer protocol. The cDNA libraries obtained were assessed using the Qubit system (Invitrogen, Carlsbad, CA) and examined for quality using Experion DNA 1 K chip (BioRad, Hercules, CA). The libraries were sequenced using NextSeq 500 High Output Kit (300 cycles-PE100) on the Illumina NextSeq 500 platform and the reads were checked for

quality using Illumina BaseSpace Onsite Computing platform. A total of 24,341 genes were sequenced, of which there were two sets of duplicates, giving a total of 24,339 analyzed (Supplemental Table 1). Validation was performed by qRT-PCR for *Il4*, *Tgfb1*, *Arg1*, *Ym1*, *Pdgfc*, and *Fam198b*, with comparisons made by regression analysis (Supplemental Fig. 3). Visualization tools provided in Metaboanalyst 3.0 (<http://www.metaboanalyst.ca>) were used to analyze clustering and correlation. Enrichment analysis for significantly different proteins was performed using Enrichr (<http://amp.pharm.msm.edu/Enrichr/>) gene ontology (GO) biological processes.

2.9. Bone marrow derived monocyte stimulation

Mononuclear cells were isolated from the femur and tibia of mice as previously described [13]. Using a 26-gauge needle and 10 mL syringe filled with RPMI 1640 media supplemented with penicillin/streptomycin and 2 mM EDTA, bone marrow cells were flushed from the bones. The cell suspension was filtered to obtain the mononuclear fraction. To obtain an adequate number of cells for stimulation, each stimulation set was pooled from three mice; the *n* reflects number of pooled sets. Monocytes (1×10^6) were stimulated with mouse recombinant IL-4 (20 ng/ml, 404-ML, R&D Systems, Minneapolis, MN), mouse recombinant PDGF-CC (10 μ g/ml, 1447-PC, R&D Systems, Minneapolis, MN), or PDGF-C antibody (200 ng/ml, AF-1447, R&D systems, Minneapolis, MN) and incubated for 2 h at 37 °C in 5% CO₂. The negative control was unstimulated cells. Following stimulation, cells were centrifuged at 400 $\times g$ for 10 min, and the cell pellets were used to measure *Arg1* and *Ym1* mRNA expression by qRT-PCR.

2.10. Re-analysis of RNA-seq datasets

We have previously collected RNA-seq data for macrophages and fibroblasts isolated from MI days 0, 1, 3, and 7. These dataset were re-analyzed for IL-4 expression in these cells [6,8]. We have also previously collected RNA-seq data for peritoneal macrophages stimulated with IL-4 (20 ng/mL for 4 h) [27]. This dataset was re-analyzed for expression of phagocytosis genes.

2.11. Statistics

Statistical analyses were performed with GraphPad Prism 8, according to the guidelines outlined in Statistical Considerations in Reporting Cardiovascular Research [28]. Experiments were conducted in a blinded manner, and results are shown as mean \pm SEM. Students *t*-test was used to compare two groups, with a value of $p < .05$ considered statistically significant. To determine differentially expressed proteins for RNA-seq data, *t*-test was used with a false discovery rate (FDR) adjusted *p* value cutoff of 0.05. RNA-seq and qRT-PCR results were compared using goodness of fit linear regression.

3. Results

3.1. MI II4 expression

Macrophages express II4r at MI days 3 and 7, while fibroblasts express II4r at MI day 3 (Supplemental Fig. 4). Macrophages express II4i1 at MI day 1, while fibroblasts did not express II4i1 through MI day 7. II4i1 is IL-4 induced protein 1 and expression indicates a

response to IL-4 [7]. This data suggest that macrophages and fibroblasts can both respond to IL-4 infusion.

3.2. IL-4 reduced cardiac inflammation after MI by deactivating the N1 pro-inflammatory phenotype in neutrophils and shifting macrophages towards an M2 anti-inflammatory phenotype

We investigated the effect of exogenous IL-4 on 11 inflammatory markers in neutrophils and macrophages isolated from d3 post MI LV. There were no differences in the total number of neutrophils ($p = .45$) and macrophages ($p = .66$) isolated from saline and IL-4 treated infarcts at MI day 3. The lack of difference could indicate that effects of the phagocytosis difference may not be evident until later times. Of note, there was a large reduction in the individual variability of neutrophil infiltration with IL-4 treatment (coefficient of variation (CV) = 74% in saline group vs. CV = 10% in IL-4 group). IL-4 treatment was started at 24 h after MI, a time when neutrophil infiltration has already reached peak levels [13,22]. Macrophage infiltration is dependent on orchestration by the neutrophils [29]; therefore, the lack of effect on cell numbers was expected.

In neutrophils, in vivo IL-4 treatment downregulated transcription of N1 pro-inflammatory markers *Ccl3*, *Il12a*, and *Tnfa* and pro-fibrotic marker *Tgfb1* (Fig. 1). In macrophages, IL-4 treatment increased anti-inflammatory *Arg1* and *Ym1*, both of which were M2 anti-inflammatory markers (Fig. 2). None of the other 7 pro- or 2- anti-inflammatory markers were different.

3.3. IL-4 had no effect on neutrophil tissue clearance rates

Tissue clearance capacity, the ability for neutrophils to breakdown gelatin, was quantified by the amount of gelatin the neutrophils could digest over a 4 h incubation period. Tissue clearance provides an assessment of total degradative capacity of neutrophils in the MI environment. There was no difference in the amount of gelatin cleared by neutrophils isolated from d3 infarcts of saline or IL-4 treated mice. The clearance rates were 0.15 ± 0.01 OD for saline ($n = 6$) and 0.17 ± 0.02 OD for IL-4 treated neutrophils ($n = 7$; $p = .22$). The result indicates IL-4 does not directly stimulate neutrophils to increase their clearance rate.

3.4. IL-4 stimulated macrophage phagocytosis of neutrophils but not cardiomyocytes

At d3 MI, the infarct region is predominantly inflammatory cells and necrotic myocytes that have not been removed. The border region was included as part of the infarct region. Because IL-4 stimulated phenotypic modulation of macrophages, we explored the influence of IL-4 treatment on macrophage phagocytosis. Macrophages from mice treated with IL-4 doubled the phagocytosis rate for neutrophils in the infarct region (Fig. 3A). Interestingly, there was no difference in cardiomyocyte phagocytosis by macrophages between control and IL-4 treated infarcts (Fig. 3B), indicating that IL-4 selectively stimulated neutrophil uptake to commence resolution of inflammation sooner.

Because the macrophage showed cell physiology modifications by IL-4, whole transcriptome evaluation was conducted on macrophages isolated from the infarct regions of IL-4 ($n = 10$) or saline ($n = 11$) treated mice (Supplemental Table 1). Out of 24,341 genes

sequenced, 2042 genes were different with IL-4 stimulation (all $p < .05$). To understand the selectivity in phagocytosis by macrophages from IL-4 treated infarcts, we evaluated genes involved in phagocytosis (Fig. 4). *Mertk* expression increased 71% in macrophages isolated from IL-4 treated infarcts ($p < .05$). In addition, *Mrc1* more than doubled, and *Fcgr2b* increased by more than 50% (both $p < .05$) with IL-4 treatment. There was no difference in the other phagocytic markers *Cd36*, *Fcgr1*, *Tubb5*, *Dynlt1a*, and *Prdx1*, indicating that phagocytosis of neutrophils is selectively regulated. *Gas6* has been reported to be critical for apoptotic neutrophil clearance by macrophages [30]. *Gas6* was 1.88 fold elevated in macrophages isolated from IL-4 treated infarcts ($p < .001$), consistent with its role. ICAM-1 has recently been shown to be a receptor for macrophage efferocytosis [31]. There was no difference between control and IL-4 stimulated macrophages ($p = .16$), indicating that *Icam1* expression in macrophages was not modified by IL-4. In vitro stimulation of macrophages with IL-4 induced *Dynlt1a*, *Fcgr2b*, *Mertk*, *Mrc1*, *Prdx*, and *Tubb5* (Fig. 5). This finding corroborates that macrophages respond directly to IL-4 to upregulate *Fcgr2b*, *Mertk*, and *Mrc1* in vitro and in vivo. Interestingly, in vitro stimulation of macrophages with IL-4 reduced *Dynlt1a* and *Prdx*, whereas in vivo expression did not change.

3.5. IL-4 stimulation shifted macrophage signaling

Of 83 interleukin genes and their receptors examined by targeted evaluation, IL-4 stimulation changed macrophage expression of 10 genes. The most prominent change was in *Il4* itself, which was elevated 5.94 fold ($p = .005$) and indicated effective overexpression. IL-4 also increased expression for: *Il13* (2.63 fold, $p = .001$), *Il1ra2* (2.52 fold, $p = .005$), *Il18bp* (1.24 fold, $p = .002$), and *Il27ra* (1.41 fold, $p = .005$). IL-4 decreased expression of *Il1b* (0.39 fold, $p = .04$), *Il6* (0.64 fold, $p = .01$), *Il1rn* (0.68 fold, $p = .001$), *Il20* (0.42 fold, $p = .04$), and *Il24* (0.32 fold, $p = .04$). These results were consistent with a shift to inflammation resolution.

Partial Least Squares Discriminant Analysis (PLSDA) revealed that IL-4 shifted macrophage polarization to a distinct profile (Fig. 6A). By Variable Importance of Projection score, *Pdgfc* was ranked the most important feature of IL-4 stimulation (Fig. 6B). By qRT-PCR, *Pdgfc* was 2.5-fold elevated in the IL-4 treated group ($p < .0001$), and the regression analysis for qRT-PCR vs. RNA-seq showed an excellent correlation ($r = 0.96$ and $p < .0001$; Supplemental Fig. 2).

To explore signaling mechanisms, a panel of 566 signaling genes was evaluated. Of the signaling genes assessed, 173 (31%) were different with IL-4 treatment (all FDR $p < .05$). Volcano plotting revealed strong upregulation of *Pdgfc*, *Lif*, *Igf2r*, and *Traf5* signaling with IL-4 treatment, concomitant with downregulation of *Ccl6*, *Ccl2*, and *Stats2* signaling contributing to the anti-inflammatory role of IL-4 (Fig. 6C). Enrichr analysis of upregulated and downregulated genes from volcano plotting uncovered a role for IL-4 in promoting macrophage positive regulation of type 2 immunity and negative regulation of phospholipases (Fig. 6D and E) [32,33].

3.6. IL-4 shifted macrophage polarization by MI day 3 without influencing cardiac physiology

IL-4 treatment administered prior to MI or started at 20 min after ligation improves cardiac structure by reducing infarct size [1,2], which indicates pre- and peri-MI IL-4 treatment strategies improve outcomes by reducing myocyte loss. Both strategies are not mechanistically informative or clinically relevant. We started IL-4 treatment 24 h after MI as a translational experimental design, beyond the time when myocardial salvage is possible [34]. Baseline d0 pre-MI echocardiograms and MI d1 assessments showed similar values between the two groups (all $p =$ not significant). At MI d3, cardiac structure and physiology remained similar between the saline and IL-4 treated groups (Table 1). There were also no differences in change from day 0 to MI d1 or d3. Infarct size was $47 \pm 2\%$ for the saline group ($n = 17$) and $45 \pm 2\%$ for the IL-4 treated group ($n = 17$, $p = .42$). The cell physiology phenotypes, therefore, precede LV changes. This was an important control to isolate cell effects from global LV effects.

3.7. Bone marrow derived monocytes stimulated with PDGF-CC protein show no difference in anti-inflammatory gene expression

Due to the strong upregulation of *Pdgfc* gene in macrophages, we examined whether IL-4 mediated its anti-inflammatory effects through *Pdgfc* signaling. Bone marrow derived monocytes stimulated with recombinant PDGF-CC protein showed no change in expression of *Arg1* or *Ym1* mRNA, and addition of a PDGF-CC blocking antibody also had no effect on *Arg1* or *Ym1* expression. IL-4 stimulation itself increased mRNA levels of both *Arg1* and *Ym1* without stimulating *Pdgfc*. Thus, IL-4 upregulated *Arg1* and *Ym1* independent of *Pdgfc* signaling, and *Pdgfc* is upregulated in MI macrophages independent of direct IL-4 stimulation. *Pdgfc* preferentially binds to *Pdgfra*, and *Pdgfra* was downregulated 0.52 fold in vivo in IL-4 treated macrophages ($p = .03$). *Pdgfrb* showed no change in expression. This indicates IL-4 may stimulate a feedback loop where reduced *Pdgfra* stimulated production of more *Pdgfc*.

Macrophages show a peak expression of *Pdgfc* on MI day 7, a time when ECM deposition by macrophages is also at its peak [6]. To explore the effect of IL-4 on macrophage dependent ECM breakdown, we examined expression of 23 MMPs and 4 tissue inhibitors of metalloproteinases (TIMPs). In vivo IL-4 stimulation increased macrophage expression of *Mmp12* (2.12 fold, $p < .0001$), *Mmp27* (1.84 fold, $p < .0001$), and *Mmp10* (1.77 fold, $p = .008$), as well as *Timp2* (2.08 fold, $p < .0001$), while decreasing expression of *Mmp14* (0.70 fold, $p = .0002$). Of 45 collagens, IL-4 stimulation reduced *Col18a1* (0.65 fold, $p = .019$) and *Col28a1* (0.32 fold, $p = .045$) without changing expression of *Fn1*, *Postn* or *Spp1*. *Pdgfc* expression, therefore, may play an important role in the ECM breakdown to deposition transition [35].

4. Discussion

The goal of this study was to evaluate the effect of exogenous IL-4 administration on in vivo inflammatory cell polarization after MI. The major findings were: 1) IL-4 promoted inflammation resolution in neutrophils while driving macrophages towards an

anti-inflammatory signature; 2) IL-4 induced macrophages to preferentially phagocytose more neutrophils without changing phagocytosis of myocytes; and 3) IL-4 induced a shift in MI macrophages to upregulate type 2 immunity and downregulate phospholipase signaling. Our results demonstrate that in vivo IL-4 treatment started 24 h after MI profoundly shifts neutrophil and macrophage polarization to initiate inflammation resolution sooner (Fig. 7).

IL-4 mediates inflammation resolution [36]. Neutrophils are the first immune cells to infiltrate the injured site following MI and have demonstrated phenotypic heterogeneity throughout the MI time course [13]. Neutrophils initiate a damaging but necessary pro-inflammatory response following MI, and it is important that this response not be impaired [29,37]. In addition, circadian rhythms have a strong influence on neutrophil actions, as neutrophils in mice given MI in the evening had exacerbated degranulation compared to neutrophils in mice given MI in the morning [38]. IL-4 treatment decreased the pro-inflammatory and pro-fibrotic cytokines *Ccl3*, *Il12a*, *Tnfa*, and *Tgfb1* in neutrophils. Macrophages, in contrast, showed upregulation of anti-inflammatory markers without effect on pro-inflammation. Consistent between our RT-PCR and RNA-seq data, in vivo IL-4 treatment of macrophages stimulated anti-inflammatory *Arg1* and *Ym1*. Both *Arg1* and *Ym1* have been shown to be important for cardiac remodeling [39,40]. Both *Ccr5* deletion and IL-10 infusion alter macrophage polarization profiles to change the cardiac wound healing landscape [19,41]. Polarization can be classified by arginine metabolism routes within the macrophage, thus balancing between pro- and anti-inflammatory activities of nitric oxide synthase and arginase [42]. The inherent ability of Ym1 binding to glucosamine and heparin/heparan sulfate may be beneficial in restructuring ECM after MI [43]. These data combined affirm that anti-inflammatory effects of IL-4 could occur by dampening pro-inflammation or enhancing anti-inflammation.

Phagocytosis is a major component of cardiac wound healing, being necessary to remove necrotic cardiomyocytes and apoptotic neutrophils [6,30]. We recently reported CXCL4 infusion significantly decreased macrophage phagocytosis of both neutrophils and myocytes to extend the wound healing process by inhibiting CD36 [17]. The current study extends our knowledge on the selectivity of macrophage phagocytosis in response to different stimuli. Here, we demonstrate for the first time that infarct macrophages from IL-4 treated mice preferentially phagocytose more neutrophils without changing myocyte rates. The absence of a change in myocyte rate also reflects the similar infarct sizes between the two groups, as myocyte damage generates the signals within the myocyte to stimulate its engulfment by macrophages. The phagocytosis genes measured may be specific to pathways designed for neutrophil phagocytosis rather than cardiomyocyte phagocytosis. It is also possible that cardiomyocytes may be protected with IL-4 treatment and thus fewer cells are being phagocytosed. Further studies regarding the possibility of selective phagocytosis in the infarct area are needed. Of the 10 phagocytic markers examined (*CD36*, *Dynt11a*, *Fcgr1*, *Fcgr2b*, *Mertk*, *Mrc1*, *Prdx2*, *Tubb5*, *Gas6*, and *Icam11*), only *Mertk*, *Mrc1*, *Fcgr2b*, and *Gas6* were elevated. This provides information on which genes selectively regulate neutrophil cell-specific uptake. In addition to upregulating phagocytic genes, IL-4 relies on *Mertk* to induce macrophages tissue repair genes using in vitro experimentation [3]. Increases in functional *Mertk* increases phagocytic capacity of macrophages and increases IL-10 production [44].

PDGF-CC did not directly stimulate *Arg1* or *Ym1* gene expression, and a PDGF-CC blocking antibody did not reduce *Arg1* or *Ym1* mRNA, revealing that *Pdgfc* was not directly responsible for the IL-4-induction of M2 polarization markers in macrophages. *Pdgfc* peaks in MI macrophages at day 7 when ECM synthesis by macrophages is also at its peak, indicating that *Pdgfc* signaling is more aligned with the ECM component than the inflammatory component of wound healing [6]. Indeed, Wiradjaja and colleagues identified *Pdgfc* as a positive regulator of ECM remodeling [45]. IL-4 in vivo stimulation upregulated *Mmp12*, *Mmp27*, and *Mmp10* as well as *Timp2*, while reducing *Mmp14*, *Col18a1*, and *Col28a1* in MI macrophages. Endostatin is a fragment of collagen 18 with anti-angiogenic activity, and endostatin treatment of pulmonary macrophages reduced expression of IL4, IL-10, IL-13, VEGF, *Arg1*, and *Ym1* [46]. IL-4, therefore, may be working through *Pdgfc* to shift the ECM landscape and indirectly promote anti-inflammation and angiogenesis. PDGF-CC also plays a role in lymphangiogenesis and blood vessel maturation and could play a role in restoring blood flow to the infarct region [47]. PDGF-CC preferentially binds to PDGFR α [48], and *Pdgfra* was downregulated by IL-4 indicating a feedback loop exists between *Pdgfra* and *Pdgfc*.

Our lab has previously reported the molecular and cellular mechanisms underlying the protective effects of IL-10, an anti-inflammatory cytokine, after MI [41]. IL-4 and IL-10 are both well-known anti-inflammatory cytokines that upregulate M2 macrophage genes, and their mechanisms of actions share mutual and distinct components. IL-4 reduced pro-inflammatory genes in the neutrophil. Both IL-4 and IL-10 activate fibroblasts to improve scar formation by promoting collagen synthesis [41,49]. IL-4 generated different responses in neutrophils (reduce pro-inflammation) and macrophages (stimulate anti-inflammation) to yield the same reduction in inflammation and induce an overall environment of pro-resolution.

Previous studies have demonstrated that IL-4 pre- or peri-MI treatment prevents the inflammatory response to MI. Our study adds to the literature on the cell biology effects of IL-4 treatment initiated after the inflammatory response has initiated. Future studies using IL-4 or IL-4 receptor null animals are needed to further define the role of IL-4 signaling in leukocyte and LV physiology. The current study contributes to the emerging knowledge of the protective effects of IL-4 following cardiac injury. Our data revealed that IL-4 turns off neutrophil N1 pro-inflammatory polarization and drives macrophages towards M2 anti-inflammatory polarization, providing new insights into the therapeutic potential of IL-4.

Supplementary Material

Refer to Web version on PubMed Central for supplementary material.

Acknowledgements

We acknowledge technical support from Elizabeth R. Flynn and Dr. Alan Mouton. Dr. Lindsey is a Stokes-Shackelford Professor at UNMC. We acknowledge funding from National Institutes of Health under Award Numbers HL075360, HL129823, HL137673, and HL137319, and from the Biomedical Laboratory Research and Development Service of the Veterans Affairs Office of Research and Development under Award Numbers 5101BX000505 and 51K2BX003922. The work performed through the UMMC Molecular and Genomics Facility is

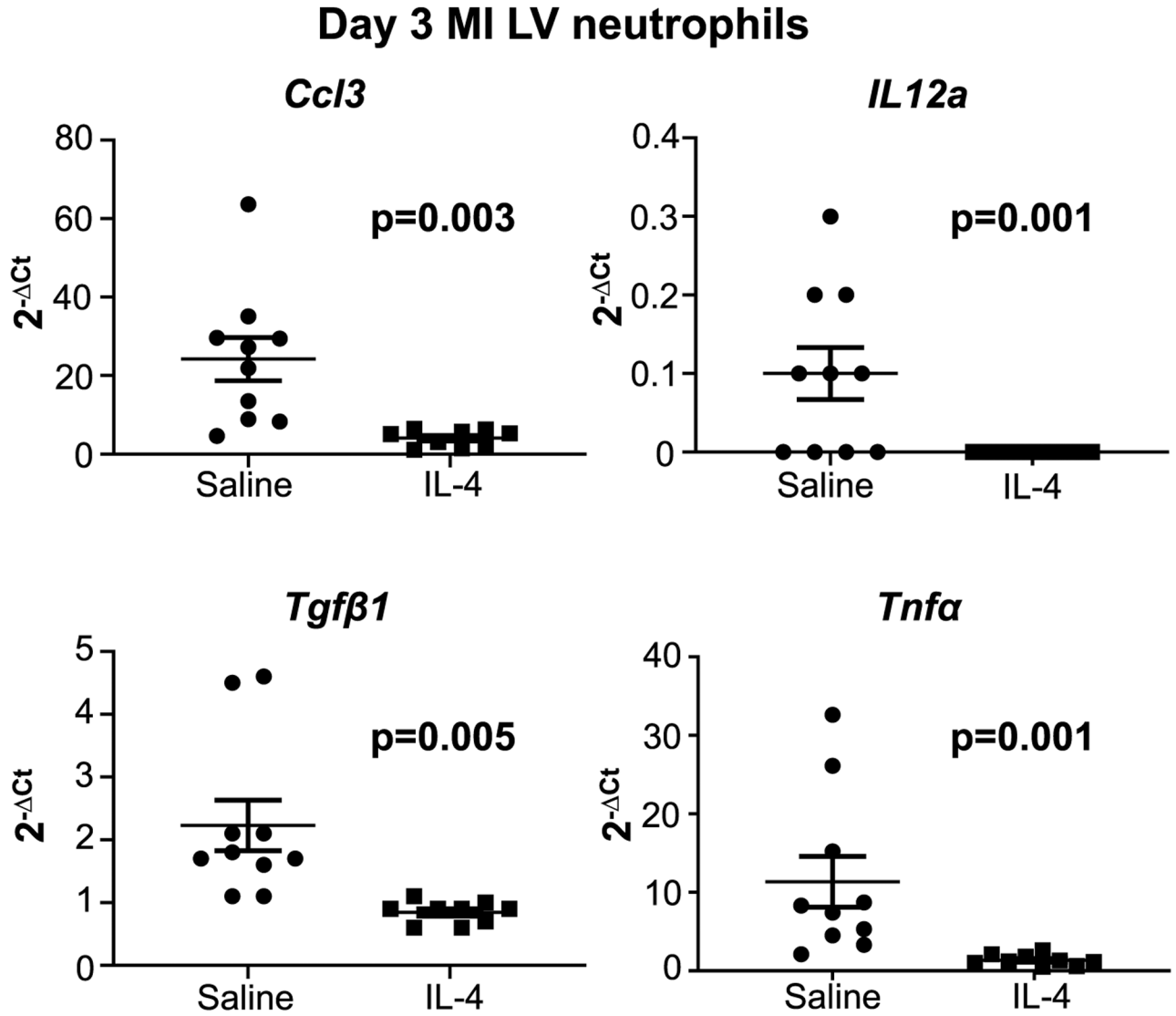
supported, in part, by funds from the NIGMS, including Mississippi INBRE (P20GM103476), Obesity, Cardiorenal and Metabolic Diseases-COBRE (P20GM104357), and Mississippi Center of Excellence in Perinatal Research (MS-CEPR)-COBRE (P20GM121334). The content is solely the responsibility of the authors and does not necessarily represent the official views of any of the funding agencies. All authors have reviewed and approved the article.

References

- [1]. Shiraishi M, Shintani Y, Shintani Y, Ishida H, Saba R, Yamaguchi A, et al. , Alternatively activated macrophages determine repair of the infarcted adult murine heart, *J. Clin. Invest* 126 (6) (2016) 2151–2166. [PubMed: 27140396]
- [2]. Shintani Y, Ito T, Fields L, Shiraishi M, Ichihara Y, Sato N, et al. , IL-4 as a repurposed biological drug for myocardial infarction through augmentation of reparative cardiac macrophages: proof-of-concept data in mice, *Sci. Rep* 7 (1) (2017) 6877. [PubMed: 28761077]
- [3]. Bosurgi L, Cao YG, Cabeza-Cabrero M, Tucci A, Hughes LD, Kong Y, et al. , Macrophage function in tissue repair and remodeling requires IL-4 or IL-13 with apoptotic cells, *Science* 356 (6342) (2017) 1072–1076. [PubMed: 28495875]
- [4]. Casella G, Garzetti L, Gatta AT, Finardi A, Maiorino C, Ruffini F, et al. , IL4 induces IL6-producing M2 macrophages associated to inhibition of neuroinflammation in vitro and in vivo, *J. Neuroinflammation* 13 (1) (2016) 139. [PubMed: 27266518]
- [5]. Seki K, Sanada S, Kudinova AY, Steinhauser ML, Handa V, Gannon J, et al. , Interleukin-33 prevents apoptosis and improves survival after experimental myocardial infarction through ST2 signaling, *Circ. Heart Fail* 2 (6) (2009) 684–691. [PubMed: 19919994]
- [6]. Mouton AJ, DeLeon-Pennell KY, Rivera Gonzalez OJ, Flynn ER, Freeman TC, Saucerman JJ, et al. , Mapping macrophage polarization over the myocardial infarction time continuum, *Basic Res. Cardiol* 113 (4) (2018) 26. [PubMed: 29868933]
- [7]. Yue Y, Huang W, Liang J, Guo J, Ji J, Yao Y, et al. , IL4I1 is a novel regulator of M2 macrophage polarization that can inhibit T cell activation via L-tryptophan and arginine depletion and IL-10 production, *PLoS One* 10 (11) (2015) e0142979. [PubMed: 26599209]
- [8]. Mouton AJ, Ma Y, Rivera Gonzalez OJ, Daseke MJ, Flynn ER, Freeman TC, et al. , Fibroblast polarization over the myocardial infarction time continuum shifts roles from inflammation to angiogenesis, *Basic Res. Cardiol* 114 (2) (2019) 6. [PubMed: 30635789]
- [9]. Lubberts E, Joosten LA, van Den Berselaar L, Helsen MM, Bakker AC, van Meurs JB, et al. , Adenoviral vector-mediated overexpression of IL-4 in the knee joint of mice with collagen-induced arthritis prevents cartilage destruction, *J. Immunol* 163 (8) (1999) 4546–4556. [PubMed: 10510398]
- [10]. Miossec P, Chomarat P, Dechanet J, Moreau JF, Roux JP, Delmas P, et al. , Interleukin-4 inhibits bone resorption through an effect on osteoclasts and pro-inflammatory cytokines in an ex vivo model of bone resorption in rheumatoid arthritis, *Arthritis Rheum.* 37 (12) (1994) 1715–1722. [PubMed: 7986216]
- [11]. DeLeon-Pennell KY, Mouton AJ, Ero OK, Ma Y, Padmanabhan Iyer R, Flynn ER, et al. , LXR/RXR signaling and neutrophil phenotype following myocardial infarction classify sex differences in remodeling, *Basic Res. Cardiol* 113 (5) (2018) 40. [PubMed: 30132266]
- [12]. Zamilpa R, Zhang J, Chiao YA, de Castro Brás LE, Halade GV, Ma Y, et al., Cardiac wound healing post-myocardial infarction: a novel method to target extracellular matrix remodeling in the left ventricle, in: Gourdie RG, Myers TA (Eds.), *Wound Regeneration and Repair: Methods and Protocols*, Humana Press, Totowa, NJ, 2013, pp. 313–324.
- [13]. Daseke MJ, Valerio FM, Kalusche WJ, Ma Y, DeLeon-Pennell KY, Lindsey ML, Neutrophil proteome shifts over the myocardial infarction time continuum, *Basic Res. Cardiol* 114 (5) (2019) 37. [PubMed: 31418072]
- [14]. Lindsey ML, Bolli R, Cauty JM Jr., Du X-J, Frangogiannis NG, Frantz S, et al. , Guidelines for experimental models of myocardial ischemia and infarction, *Am. J. Physiol. Heart Circ. Physiol* 314 (4) (2018) H812–H838. [PubMed: 29351451]

- [15]. Iyer RP, de Castro Brás LE, Cannon PL, Ma Y, DeLeon-Pennell KY, Jung M, et al. , Defining the sham environment for post-myocardial infarction studies in mice, *Am. J. Physiol. Heart Circulat. Physiol* 311 (3) (2016) H822–H836.
- [16]. Lindsey ML, Kassiri Z, Virag JAI, Brás LEDC, Scherrer-Crosbie M, Guidelines for measuring cardiac physiology in mice, *Am. J. Physiol. Heart Circulat. Physiol* 314 (4) (2018) H733–H752.
- [17]. Lindsey ML, Jung M, Yabluchanskiy A, Cannon PL, Iyer RP, Flynn ER, et al. , Exogenous CXCL4 infusion inhibits macrophage phagocytosis by limiting CD36 signalling to enhance post-myocardial infarction cardiac dilation and mortality, *Cardiovasc. Res* 115 (2) (2019) 395–408. [PubMed: 30169632]
- [18]. Ma Y, Chiao YA, Zhang J, Manicone AM, Jin Y-F, Lindsey ML, Matrix metalloproteinase-28 deletion amplifies inflammatory and extracellular matrix responses to cardiac aging, *Microsc. Microanal* 18 (1) (2012) 81–90. [PubMed: 22153350]
- [19]. Zamilpa R, Kanakia R, Joaquin Cigarroa I, Dai Q, Escobar GP, Martinez H, et al. , CC chemokine receptor 5 deletion impairs macrophage activation and induces adverse remodeling following myocardial infarction, *Am. J. Phys. Heart Circ. Phys* 300 (4) (2011) H1418–H1426.
- [20]. Zamilpa R, Ibarra J, de Castro Brás LE, Ramirez TA, Nguyen N, Halade GV, et al. , Transgenic overexpression of matrix metalloproteinase-9 in macrophages attenuates the inflammatory response and improves left ventricular function post-myocardial infarction, *J. Mol. Cell. Cardiol* 53 (5) (2012) 599–608. [PubMed: 22884843]
- [21]. Ma Y, Mouton AJ, Lindsey ML, Cardiac macrophage biology in the steady-state heart, the aging heart, and following myocardial infarction, *Transl. Res* 191 (2018) 15–28. [PubMed: 29106912]
- [22]. Ma Y, Yabluchanskiy A, Iyer RP, Cannon PL, Flynn ER, Jung M, et al. , Temporal neutrophil polarization following myocardial infarction, *Cardiovasc. Res* 110 (1) (2016) 51–61. [PubMed: 26825554]
- [23]. Ma Y, Chiao YA, Clark R, Flynn ER, Yabluchanskiy A, Ghasemi O, et al. , Deriving a cardiac ageing signature to reveal MMP-9-dependent inflammatory signalling in senescence, *Cardiovasc. Res* 106 (3) (2015) 421–431. [PubMed: 25883218]
- [24]. Nahrendorf M, Swirski FK, Abandoning M1/M2 for a network model of macrophage function, *Circ. Res* 119 (3) (2016) 414–417. [PubMed: 27458196]
- [25]. Jiménez VC, Bradley EJ, Willemsen AM, Kampen AHC, Baas F, Kootstra NA, Next-generation sequencing of microRNAs uncovers expression signatures in polarized macrophages, *Physiol. Genom* 46 (3) (2014) 91–103.
- [26]. Liu GW, Livesay BR, Kacherovsky NA, Cieslewicz M, Lutz E, Waalkes A, et al. , Efficient identification of murine M2 macrophage peptide targeting ligands by phage display and next-generation sequencing, *Bioconjug. Chem* 26 (8) (2015) 1811–1817. [PubMed: 26161996]
- [27]. Liu X, Zhang J, Zeigler AC, Nelson AR, Lindsey ML, Saucerman JJ, Network analysis reveals a distinct axis of macrophage activation in response to conflicting inflammatory cues, *bioRxiv* (2019) 844464.
- [28]. Lindsey ML, Gray GA, Wood SK, Curran-Everett D, Statistical considerations in reporting cardiovascular research, *Am. J. Phys. Heart Circ. Phys* 315 (2) (2018) H303–H313.
- [29]. Horckmans M, Ring L, Duchene J, Santovito D, Schloss MJ, Drechsler M, et al. , Neutrophils orchestrate post-myocardial infarction healing by polarizing macrophages towards a reparative phenotype, *Eur. Heart J* 38 (3) (2017) 187–197. [PubMed: 28158426]
- [30]. Nepal S, Tirupathi C, Tsukasaki Y, Farahany J, Mittal M, Rehman J, et al. , STAT6 induces expression of Gas6 in macrophages to clear apoptotic neutrophils and resolve inflammation, *Proc. Natl. Acad. Sci* 116 (33) (2019) 16513–16518. [PubMed: 31363052]
- [31]. Wiesolek HL, Bui TM, Lee JJ, Dalal P, Finkielstein A, Batra A, et al. , ICAM-1 functions as an efferocytosis receptor in inflammatory macrophages, *Am. J. Pathol* (2020) <https://pubmed.ncbi.nlm.nih.gov/32035057/>.
- [32]. Ilatovskaya DV, Pitts C, Clayton J, Domondon M, Troncoso M, Pippin S, et al. , CD8+ T-cells negatively regulate inflammation post-myocardial infarction, *Am. J. Phys. Heart Circ. Phys* 317 (3) (2019) H581–H596.
- [33]. Ilatovskaya DV, Halade GV, DeLeon-Pennell KY, Adaptive immunity-driven inflammation and cardiovascular disease, *Am. J. Phys. Heart Circ. Phys* 317 (6) (2019) H1254–H1257.

- [34]. Ortiz-Pérez JT, Lee DC, Meyers SN, Davidson CJ, Bonow RO, Wu E, Determinants of myocardial salvage during acute myocardial infarction: evaluation with a combined angiographic and CMR myocardial salvage index, *JACC Cardiovasc. Imaging* 3 (5) (2010) 491–500. [PubMed: 20466344]
- [35]. Han J, Li L, Zhang Z, Xiao Y, Lin J, Zheng L, et al. , Platelet-derived growth factor C plays a role in the branchial arch malformations induced by retinoic acid, *Birth Defect. Res. A* 79 (3) (2007) 221–230.
- [36]. Chatterjee P, Chiasson VL, Bounds KR, Mitchell BM, Regulation of the anti-inflammatory cytokines interleukin-4 and interleukin-10 during pregnancy, *Front. Immunol* 5 (253) (2014).
- [37]. Puhl SL, Steffens S, Neutrophils in post-myocardial infarction inflammation: damage vs. resolution? *Front. Cardiovasc. Med* 6 (2019) 25. [PubMed: 30937305]
- [38]. Schloss MJ, Horckmans M, Nitz K, Duchene J, Drechsler M, Bidzhekov K, et al. , The time-of-day of myocardial infarction onset affects healing through oscillations in cardiac neutrophil recruitment, *EMBO Mol. Med* 8 (8) (2016) 937–948. [PubMed: 27226028]
- [39]. Wynn TA, Vannella KM, Macrophages in tissue repair, *Regen. Fibros. Immun* 44 (3) (2016) 450–462.
- [40]. Peranzoni E, Marigo I, Dolcetti L, Ugel S, Sonda N, Taschin E, et al. , Role of arginine metabolism in immunity and immunopathology, *Immunobiology* 212 (9–10) (2007) 795–812. [PubMed: 18086380]
- [41]. Jung M, Ma Y, Iyer RP, DeLeon-Pennell KY, Yabluchanskiy A, Garrett MR, et al. , IL-10 improves cardiac remodeling after myocardial infarction by stimulating M2 macrophage polarization and fibroblast activation, *Basic Res. Cardiol* 112 (3) (2017) 33. [PubMed: 28439731]
- [42]. Thomas AC, Mattila JT, “Of mice and men”: arginine metabolism in macrophages, *Front. Immunol* 5 (2014) 479. [PubMed: 25339954]
- [43]. Sun YJ, Chang NC, Hung SI, Chang AC, Chou CC, Hsiao CD, The crystal structure of a novel mammalian lectin, Ym1, suggests a saccharide binding site, *J. Biol. Chem* 276 (20) (2001) 17507–17514. [PubMed: 11278670]
- [44]. DeBerge M, Yeap XY, Dehn S, Zhang S, Grigoryeva L, Misener S, et al. , MerTK cleavage on resident cardiac macrophages compromises repair after myocardial ischemia reperfusion injury, *Circ. Res* 121 (8) (2017) 930–940. [PubMed: 28851810]
- [45]. Wiradjaja F, Cottle DL, Jones L, Smyth I, Regulation of PDGFC signalling and extracellular matrix composition by FREM1 in mice, *Dis. Models Mech* 6 (6) (2013) 1426–1433.
- [46]. Foguer K, Braga Mde S, Peron JP, Bortoluci KR, Bellini MH, Endostatin gene therapy inhibits intratumoral macrophage M2 polarization, *Biomed. Pharmacother* 79 (2016) 102–111. [PubMed: 27044818]
- [47]. Reigstad LJ, Sande HM, Fluge Ø, Bruland O, Muga A, Varhaug JE, et al. , Platelet-derived growth factor (PDGF)-C, a PDGF family member with a vascular endothelial growth factor-like structure, *J. Biol. Chem* 278 (19) (2003) 17114–17120. [PubMed: 12598536]
- [48]. Li X, Pontén A, Aase K, Karlsson L, Abramsson A, Uutela M, et al. , PDGF-C is a new protease-activated ligand for the PDGF α -receptor, *Nat. Cell Biol* 2 (5) (2000) 302–309. [PubMed: 10806482]
- [49]. Aoudjehane L, Pissaia A Jr., Scatton O, Podevin P, Massault PP, Chouzenoux S, et al. , Interleukin-4 induces the activation and collagen production of cultured human intrahepatic fibroblasts via the STAT-6 pathway, *Lab. Investig* 88 (9) (2008) 973–985. [PubMed: 18626468]

**Fig. 1.**

In vivo IL-4 infusion inhibited neutrophil expression of N1 pro-inflammatory markers at day 3 MI. Neutrophils were isolated at day 3 MI from saline and IL-4 treated mice. Of the pro-inflammatory and anti-inflammatory markers evaluated, *Ccl3*, *Il12a*, *Tgfb1*, and *Tnfa* were all reduced following IL-4 treatment. $n = 11$ saline and $n = 10$ IL-4 treated mice, analyzed using Student's *t*-test.

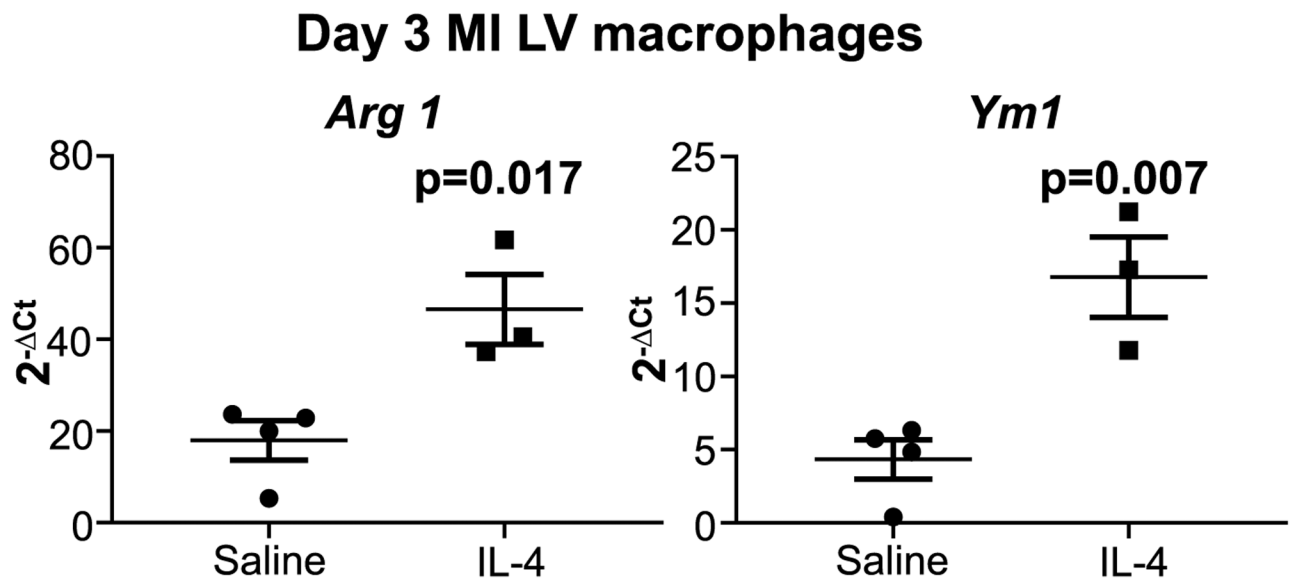


Fig. 2.

In vivo IL-4 infusion upregulated macrophage expression of M2 anti-inflammatory markers at day 3 MI. Macrophages were isolated at day 3 MI from saline and IL-4 treated mice. Of the pro-inflammatory and anti-inflammatory markers evaluated, *Arg1* and *Ym1* were increased following IL-4 treatment. $n = 4$ saline and $n = 3$ IL-4 treated, analyzed using Student's *t*-test.

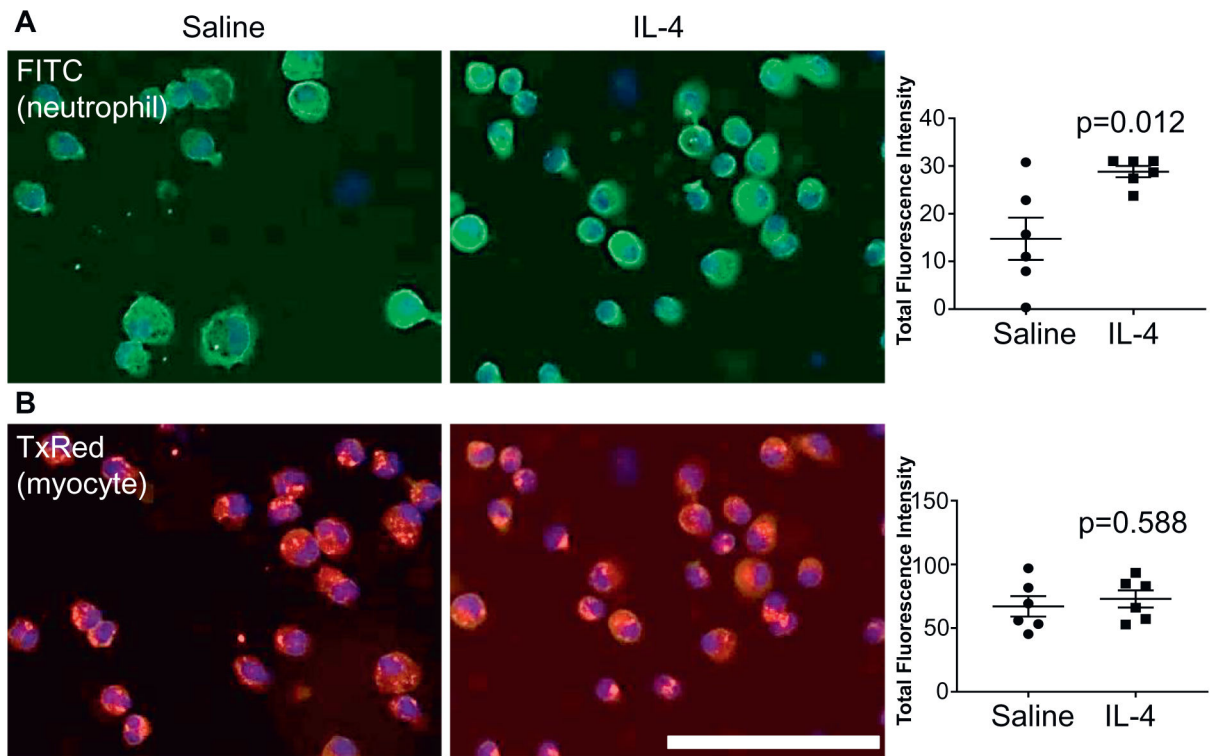


Fig. 3.

Macrophage phagocytosis of neutrophils, but not cardiomyocytes, increased with IL-4 treatment. Saline or IL-4 infusion was started at MI 1 day, and macrophages isolated from the infarct region at day 3. Ex vivo, macrophages were plated onto glass coverslips and stained for myocytes with an alpha actinin antibody and Texas Red conjugated secondary and for neutrophils with a neutrophil antibody and FITC conjugated secondary. Staining with 4',6-diamidino-2-phenylindole (DAPI) was used to stain nuclei. Representative images on the left and graphed values on the right. Values are fluorescent intensity, indicating the FITC or Texas Red positivity within the cytoplasm. Scale bar is 100 μm . $n = 6$ saline and $n = 6$ IL-4 treated, analyzed using Student's t -test. (For interpretation of the references to colour in this figure legend, the reader is referred to the web version of this article.)

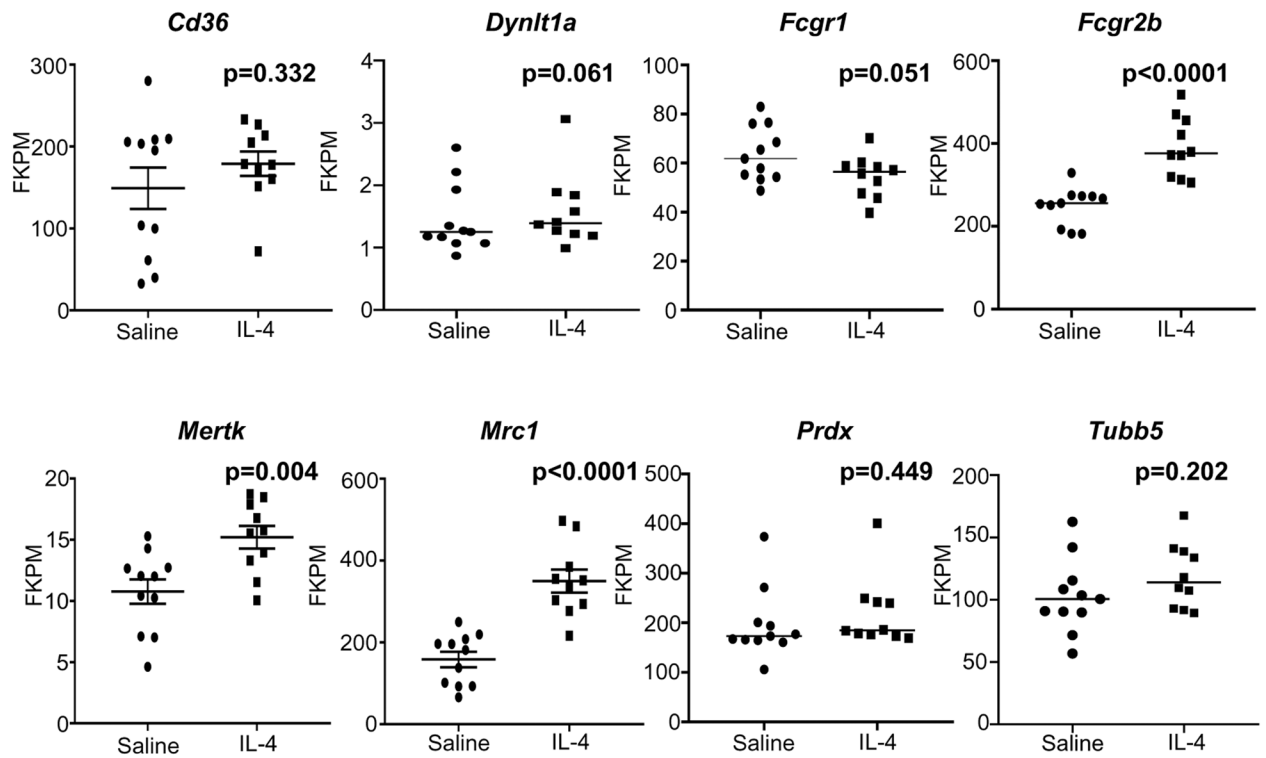


Fig. 4.

IL-4 increased macrophage phagocytosis genes *Fcgr2b*, *Mertk*, and *Mrc1* at day 3 MI. RNA-seq performed on macrophages isolated from the infarct region shows that *Fcgr2b*, *Mertk*, and *Mrc1* are all increased at MI day 3. *Cd36*, *Dynl1a*, *Fcgr1*, *Prdx*, and *Tubb5* were not different. $n = 11$ saline and $n = 10$ IL-4 treated mice, analyzed by *t*-test with a false discovery rate (FDR) adjusted p value cutoff of 0.05.

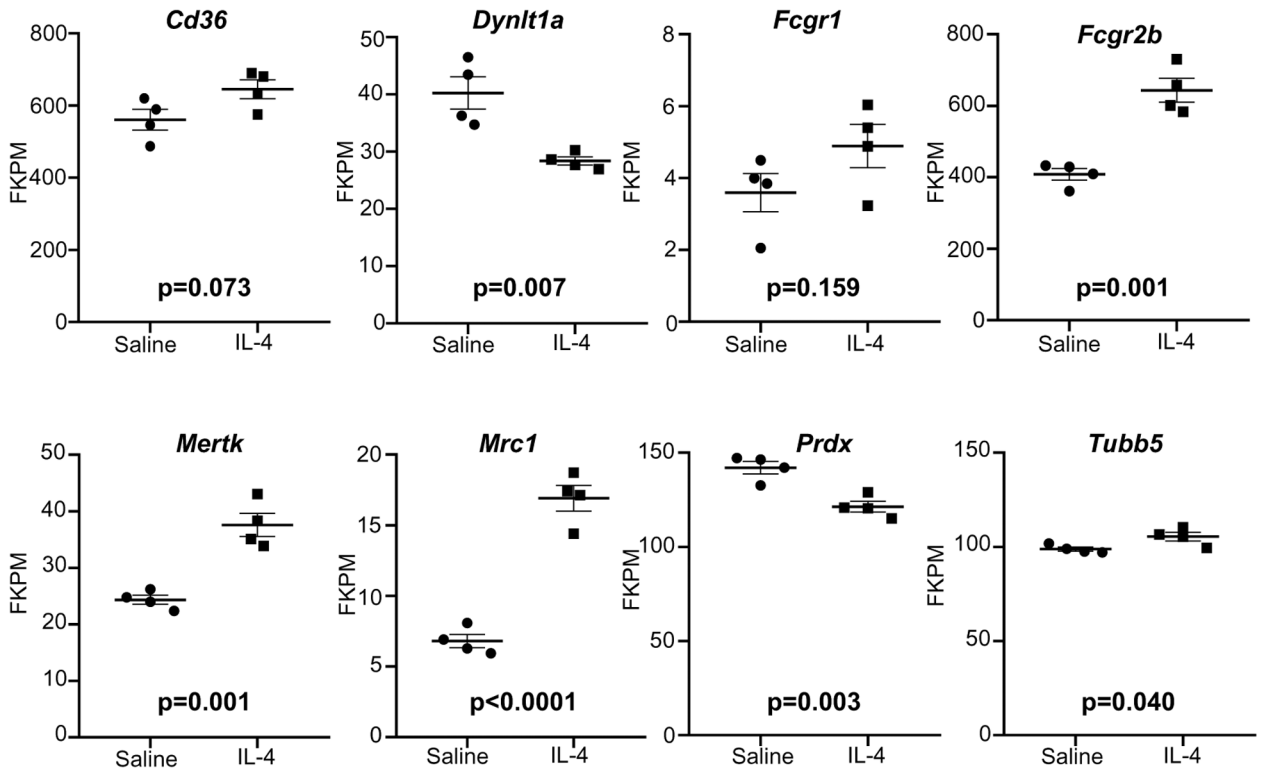


Fig. 5.

IL-4 increased macrophage phagocytosis genes in peritoneal macrophages in vitro.

Macrophages stimulated with IL-4 (20 ng/mL for 4 h) and analyzed by RNA-seq showed that *Dynlt1a*, *Fcgr2b*, *Mertk*, *Mrc1*, *Prdx*, and *Tubb5* increased with stimulation. $n = 4$ saline and $n = 4$ IL-4 treated samples, analyzed by t -test with a false discovery rate (FDR) adjusted p value cutoff of 0.05.

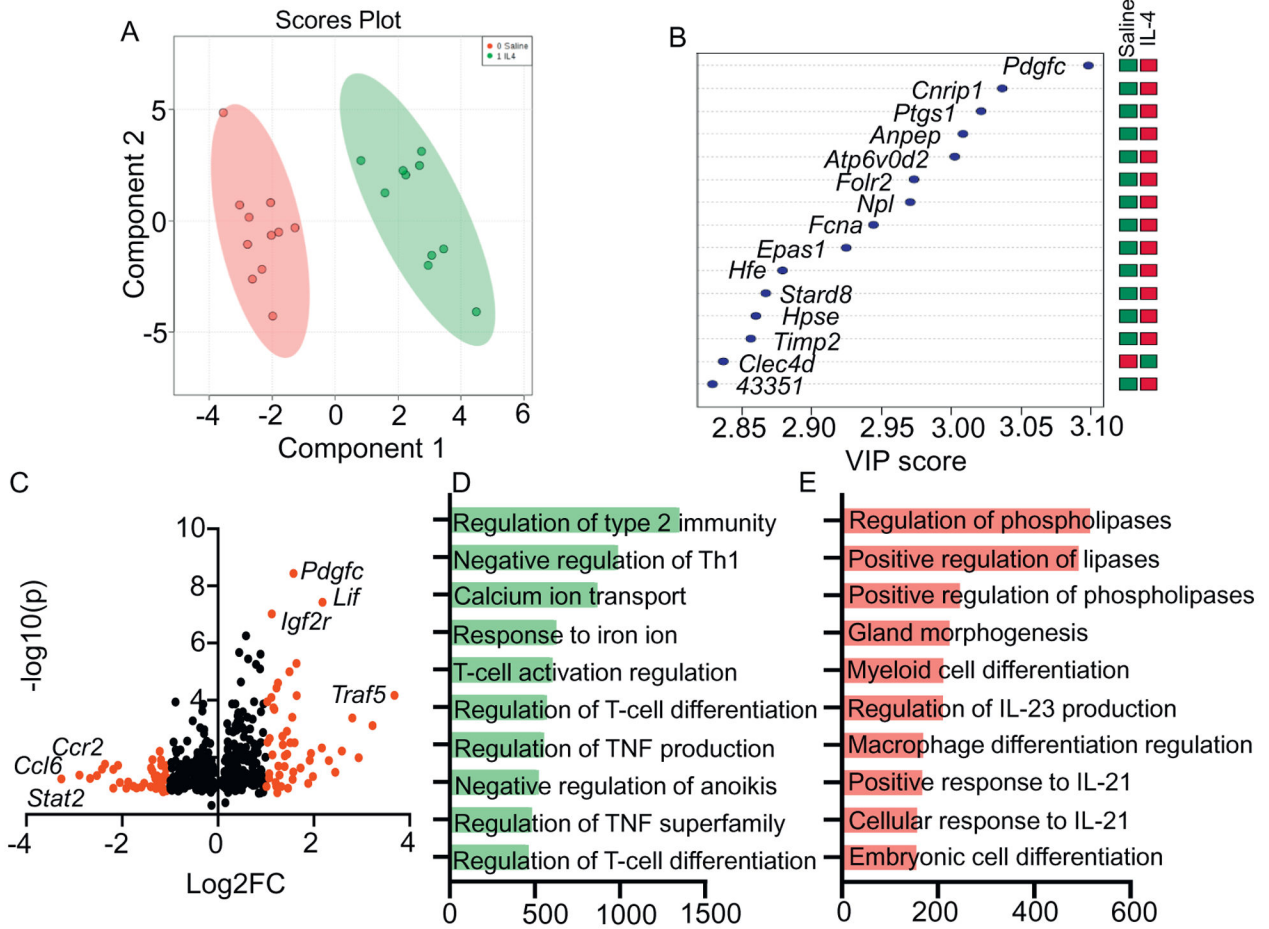
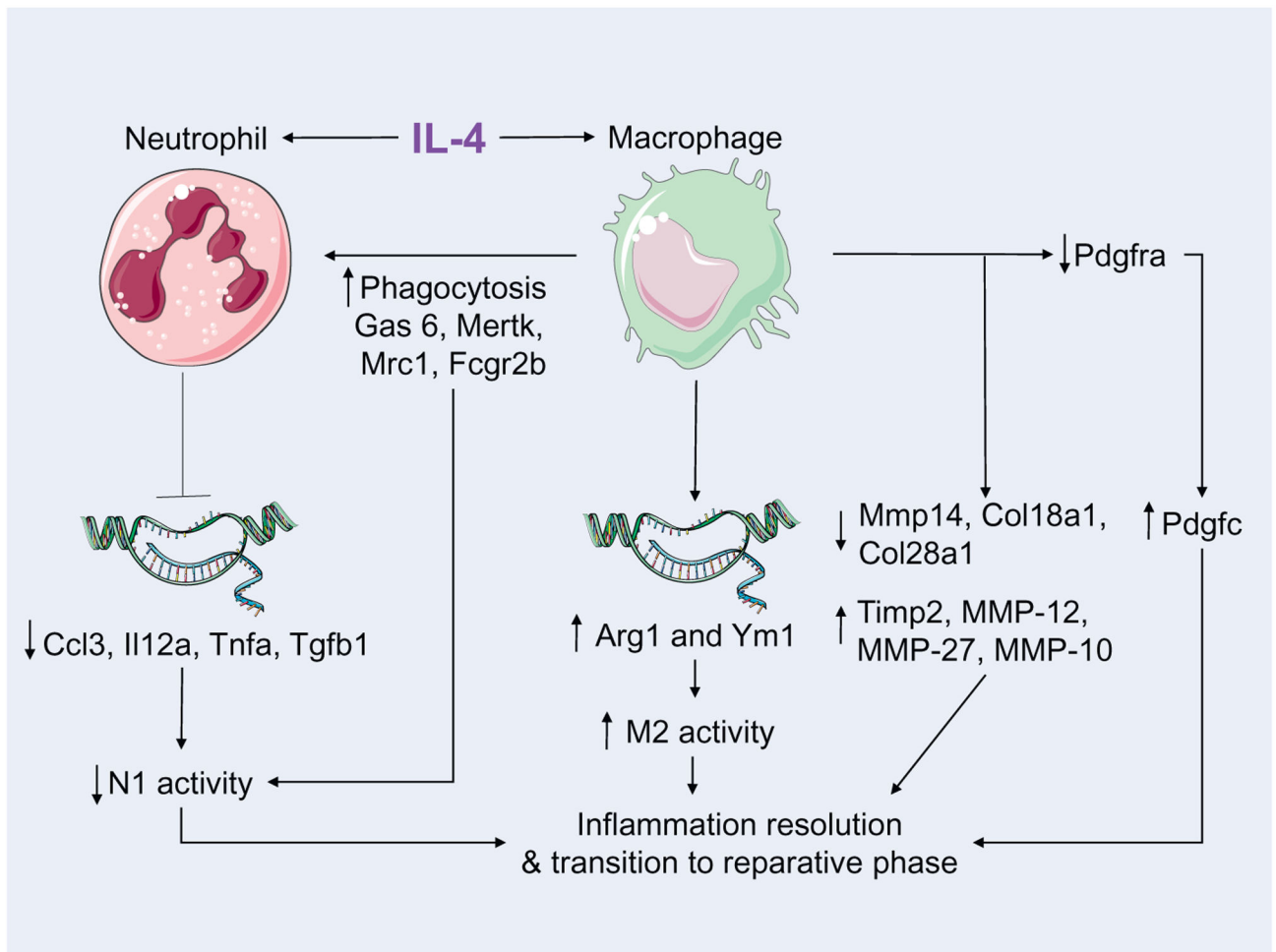


Fig. 6. IL-4 shifted macrophage polarization and signaling at MI day 3. A) Partial least squares-discriminant analysis showed no overlap between the saline (red) and IL-4 treated (green) macrophage principal component profiles. B) By Variable Importance in Projection (VIP) score, *Pdgfc* was the first ranked gene. C) From a sub-panel of 566 immunology signaling genes, volcano plotting revealed strong upregulation of *Pdgfc*, *Lif*, *Igf2r*, and *Traf5* signaling and downregulation of *Ccl6*, *Ccl2*, and *Stat2* signaling with IL-4 treatment. D and E) Enrichr analysis of upregulated (D) and downregulated (E) genes from volcano plotting uncovered a role for IL-4 in promoting macrophage positive regulation of type 2 immunity and negative regulation of phospholipases.

**Fig. 7.**

IL-4 reduced N1 pro-inflammatory genes in neutrophils, upregulated M2 anti-inflammatory genes in macrophages, and induced selective phagocytosis of neutrophils by macrophages. Flowchart summarizing the beneficial effects of IL-4 in resolving MI inflammation. All genes described are derived from RNA-Seq or qRT-PCR data.

Table 1

Echocardiography and necropsy

	Saline		IL-4		Saline		IL-4		p value
	Day 0	Day 3	Day 0	Day 3	MI day 3	MI day 3	MI day 3		
Heart rate (bpm)	484 ± 15	494 ± 5	494 ± 5	520 ± 15	506 ± 7	506 ± 7	506 ± 7	0.39	
Infarct wall thickness (mm; diastole)	1.06 ± 0.04	1.03 ± 0.03	1.03 ± 0.03	0.46 ± 0.04	0.47 ± 0.04	0.47 ± 0.04	0.47 ± 0.04	0.84	
End diastolic volume (μl)	60 ± 3	63 ± 3	63 ± 3	84 ± 3	85 ± 3	85 ± 3	85 ± 3	0.91	
End systolic volume (μl)	23 ± 1	23 ± 3	23 ± 3	64 ± 3	62 ± 3	62 ± 3	62 ± 3	0.73	
Ejection fraction (%)	62 ± 1	64 ± 1	64 ± 1	24 ± 2	26 ± 3	26 ± 3	26 ± 3	0.43	
Infarct area (%)	0	NA	NA	47 ± 2	45 ± 2	45 ± 2	45 ± 2	0.42	
LV mass (mg)	NA	NA	NA	117 ± 3	119 ± 1	119 ± 1	119 ± 1	0.54	
Lung wet weight (mg)	NA	NA	NA	180 ± 19	166 ± 8	166 ± 8	166 ± 8	0.54	

Values are mean ± SEM. bpm=beats per minute; analysis by Students *t*-test for MI day 3 comparisons; n = 6–17/group. NA-not applicable for day 0 baseline echocardiograms.